Sphingosine kinase regulates oxidized low density lipoprotein-mediated calcium oscillations and macrophage survival

Johnny H. Chen, Maziar Riazy, Shih Wei Wang, Jiazhen Minnie Dai, Vincent Duronio, and Urs P. Steinbrecher[1]

Department of Medicine, University of British Columbia, Vancouver, Canada

Abstract **We recently reported that oxidized LDL (oxLDL) induces an oscillatory increase in intracellular calcium ($[Ca^{2+}]_i$) levels in macrophages. Furthermore, we have shown that these $[Ca^{2+}]_i$ oscillations mediate oxLDL's ability to inhibit macrophage apoptosis in response to growth factor deprivation. However, the signal transduction pathways by which oxLDL induces $[Ca^{2+}]_i$ oscillations have not been elucidated. In this study, we show that these oscillations are mediated in part by intracellular mechanisms, as depleting extracellular Ca^{2+} did not completely abolish the effect. Inhibiting sarco-endoplasmic reticulum ATPase (SERCA) completely blocked $[Ca^{2+}]_i$ oscillations, suggesting a role for Ca^{2+} reuptake by the ER. The addition of oxLDL resulted in an almost immediate activation of sphingosine kinase (SK), which can increase sphingosine-1-phosphate (S1P) levels by phosphorylating sphingosine. Moreover, S1P was shown to be as effective as oxLDL in blocking macrophage apoptosis and producing $[Ca^{2+}]_i$ oscillations. This suggests that the mechanism in which oxLDL generates $[Ca^{2+}]_i$ oscillations may be *1*) activation of SK, *2*) SK-mediated increase in S1P levels, *3*) S1P-mediated Ca^{2+} release from intracellular stores, and *4*) SERCA-mediated Ca^{2+} reuptake back into the ER.**—Chen, J. H., M. Riazy, S. W. Wang, J. M. Dai, V. Duronio, and U. P. Steinbrecher. **Sphingosine kinase regulates oxidized low density lipoprotein-mediated calcium oscillations and macrophage survival. *J. Lipid Res.* 2010.** 51: **991–998.**

Supplementary key words sphingosine-1-phosphate • calcium • foam cells • plaque stability

Atherosclerosis is a chronic inflammatory disease of large and medium-sized arteries, and macrophages play a central role in its initiation and progression (1, 2). The accumulation of macrophages in lesions is due in part to recruitment of monocytes from the bloodstream (2) and to proliferation of macrophages within atherosclerotic lesions (3–6). Oxidized LDL (oxLDL) plays an important role in atherogenesis, in part because of its effects on macrophage recruitment and retention (7, 8). Initial oxidation of LDL and formation of what is often referred to as "minimally modified" LDL stimulate adjacent endothelial and smooth muscle cells to release monocyte chemotactic protein-1, which facilitates the recruitment of monocytes into the arterial wall. OxLDL itself is chemotactic for monocytes by virtue of its lysophosphatidylcholine content.

At high concentrations, oxLDL can be toxic to cultured macrophages and other cells, but at lower concentrations, it has been clearly shown to promote macrophage proliferation and inhibit apoptosis (9–15). Our group has recently reported that oxLDL inhibits macrophage apoptosis by activating eukaryotic elongation factor-2 (eEF2) kinase (also known as Ca^{2+}/calmodulin-dependent kinase III) (16). eEF2 kinase activation and inhibition of macrophage apoptosis is mediated by an oscillatory increase in intracellular calcium ($[Ca^{2+}]_i$). However, the signal transduction pathways involved in oxLDL-mediated $[Ca^{2+}]_i$ oscillations have not been elucidated.

Ca^{2+} is a ubiquitous intracellular signal responsible for controlling numerous cellular processes. These processes range from muscle contraction to synaptic transmission and from cellular proliferation to apoptosis (17). Ca^{2+} can relay specificity in signaling through its high degree of spatial and temporal diversity (18). Ca^{2+} released into the cytoplasm can function as a second messenger that can

Abbreviations: BMDM, bone marrow-derived macrophage; $[Ca^{2+}]_i$, intracellular calcium; DPBS, Dulbecco's phosphate-buffered saline; eEF2, eukaryotic elongation factor-2; ER, endoplasmic reticulum; IP_3R, inositol-1,4,5-triphosphate receptor; LCM, L929 cell conditioned media; lysoPC, lysophosphatidylcholine; MAPK, mitogen-activated protein kinase; MTS, 3-(4,5-dimethylthiazol-2-yl)-5-(3-carboxymethoxyphenyl)-2-(4-sulfophenyl)-2H-tetrazolium, inner salt; oxLDL, oxidized low density lipoprotein; PC, phosphatidylcholine; PLC, phospholipase C; PMS, phenazine methosulfate; RyR, ryanodine receptor; S1P, sphingosine-1-phosphate; SCaMPER, sphingolipid Ca^{2+} release mediating protein of the endoplasmic reticulum; SERCA, sarco-endoplasmic reticulum ATPase; SK, sphingosine kinase; SKI, sphingosine kinase inhibitor.

[1]To whom correspondence should be addressed.
e-mail: usteinbr@interchange.ubc.ca

Manuscript received 20 October 2009 and in revised form 5 November 2009.
Published, JLR Papers in Press, November 5, 2009
DOI 10.1194/jlr.M000398

mediate cell survival or induce apoptosis (19). Within the same cell, Ca^{2+} signals can have dual roles in response to the same stimulus, depending on the temporal pattern of the Ca^{2+} elevations. For example, distinct temporal patterns of Ca^{2+} elevation are associated with positive versus negative selection of developing T-cells in the thymus (20, 21). Weak T-cell receptor activation induces Ca^{2+} oscillations, whereas strong T-cell receptor activation induces sustained Ca^{2+} elevation. The former activates nuclear factor of activated T-cells optimally and thereby upregulates expression of the prosurvival cytokine IL-2, whereas the latter upregulates the proapoptotic BH3-only protein Bim.

Spingosine-1-phosphate (S1P) plays an important role in many cellular processes, including regulation of Ca^{2+} signals (22–26) and cell survival and proliferation (27–35). Intracellular levels of S1P are tightly regulated by the equilibrium between its formation, which is catalyzed by sphingosine kinase (SK), and its degradation, which is catalyzed by S1P lyase and S1P phosphatases (36). S1P produced in response to agonists has the ability to function intracellularly as a second messenger or after secretion in an autocrine/paracrine fashion to activate S1P receptors (formerly known as endothelial differentiation gene or Edg receptors) on the cell surface (37). Although S1P is thought to mobilize $[Ca^{2+}]_i$ via interaction with its surface receptors, increasing evidence suggests an important intracellular role for S1P in mediating Ca^{2+} increases within the cell (38, 39). However, the exact mechanism in which S1P mediates Ca^{2+} mobilization is still uncertain.

In this study, we describe a mechanism in which oxLDL generates $[Ca^{2+}]_i$ oscillations by *1*) oxLDL-mediated activation of SK, *2*) SK-mediated increase in S1P levels, *3*) S1P-mediated Ca^{2+} release from intracellular stores, and *4*) sarco-endoplasmic reticulum ATPase (SERCA)-mediated Ca^{2+} reuptake back into the endoplasmic reticulum (ER).

MATERIALS AND METHODS

Materials

DMEM, FBS, Dulbecco's phosphate buffered saline (DPBS), HEPES, Fluo-4-AM, pluronic acid, and propidium iodide were purchased from Invitrogen (Burlington, ON, Canada). The 3-(4,5-dimethylthiazol-2-yl)-5-(3-carboxymethoxyphenyl)-2-(4-sulfophenyl)-2H-tetrazolium, inner salt (MTS) was from Promega (Madison, WI). Phenazine methosulfate (PMS), phosphatidylcholine (PC), lysophosphatidylcholine (lysoPC), and sphingomyelin were obtained from Sigma-Aldrich (St. Louis, MO). The SK inhibitor 2-(*p*-hydroxyanilino)-4-(*p*-chlorophenyl) thiazole (SKI), U-73122, and hydrated 1-(((5-(4-nitrophenyl)-2-furanyl)-methylene)-amino)-2,4-imidazolidinedione sodium salt (dantrolene) were purchased from Calbiochem (San Diego, CA). Protein A Sepharose beads, L-[^{35}S]methionine, and L-[4,5-^{3}H] leucine were from Amersham Biosciences (Piscataway, NJ). [^{32}P] ATP was from Perkin-Elmer (Waltham, MA). BCA protein assay reagents, BSA standards, and SuperSignal Femto substrate were purchased from Pierce (Milwaukee, WI). Goat anti-rabbit IgG horseradish peroxidase-conjugated secondary antibody was from DAKO Diagnostics (Mississauga, ON, Canada). G60 silica gel plates were from Whatman (Piscataway, NJ). SDS-PAGE molecular weight standards and polyvinylidine difluoride membranes were provided by Bio-Rad (Hercules, CA). BioMax MR film was from Kodak (Rochester, NY).

Lipoprotein isolation and oxidation

LDL (d = 1.019-1.063 g/ml) was isolated from EDTA-anticoagulated whole blood of fasting healthy normolipidemic donors (15). Copper oxidation was performed by incubating LDL (200 μg/ml) with 5 μmol/l $CuSO_4$ in DPBS containing 0.90 mmol/l $CaCl_2$ and 0.49 mmol/l $MgCl_2$ for 24 h at 37°C. The reaction was stopped by addition of 40 μmol/l butylated hydroxytoluene and 300 μmol/l EDTA. The oxidized LDL was then washed and concentrated to ~1.5 mg/ml using Amicon Centricon Plus-20 ultrafilters (Millipore, Bedford, MA). After a 0.45 micron filtration, protein concentration of oxLDL was determined using BCA protein assay.

Relative electrophoretic mobility (R_f) of modified lipoproteins was assessed using a Ciba-Corning (East Walpole, MA) electrophoresis apparatus and Titan agarose gels (Beaumont, TX) in 50 mmol/l barbital buffer, pH 8.6, according to the manufacturer's instructions. BSA was added to lipoprotein samples to ensure reproducible migration distances. Lipoprotein bands were visualized by staining with Fat Red 7B. All oxLDLs used in this study was extensively modified with an R_f value $\geq$ 3 when compared with nLDL.

Cell culture

L929 cells (kindly provided by Dr. J. W. Schrader, Biomedical Research Centre, BC, Canada) were seeded in TufRol™ roller bottles (BD Falcon, San Jose, CA) at a density of 1.5×10^4 cells per cm^2 and cultured in media (DMEM, 10% FBS, 2 mmol/l L-glutamine, 1 mmol/l sodium pyruvate, 50 U/ml penicillin, and 50 μg/ml streptomycin) containing 20 mmol/l HEPES at 37°C in a 5% CO_2 atmosphere. After 15 days, the media were harvested and centrifuged at 800 *g* for 10 min. The supernatant was filter sterilized through a 0.22 μm filter. This L929 cell conditioned media (LCM) contains ~10,000 U/ml of M-CSF (40).

Bone marrow cells were obtained from the femurs of 6–8 week old female CD1 mice (Charles River Laboratories, Wilmington, MA) as previously described (15). Cells were cultured in media containing 10% LCM for 18 h at 37°C in a 95% humidity atmosphere containing 5% CO_2. After 18 h, nonadherent cells were isolated and differentiated into macrophages by culturing them in medium containing 10% LCM until 80% confluence was reached (5–6 days). Cells were washed to remove nonadherent cells and harvested using a rubber cell scraper (Sarstedt, Montreal, QC, Canada).

Calcium imaging

Bone marrow-derived macrophages (BMDMs) were seeded in 6-well plates at 5.0×10^4 cells per cm^2 and grown for 24 h. Cells were then washed with Ca^{2+}-free DPBS and incubated in Ca^{2+}-free, HEPES-buffered DPBS containing 2 μmol/l Fluo-4-AM for 30 min at room temperature. Fluo-4-AM was dissolved with 20% pluronic acid in DMSO to make a 2 mmol/l stock solution. Cells were washed again with DPBS and incubated in HEPES-buffered medium with inhibitors where indicated for 10 min at room temperature to allow for deesterification of the acetoxymethyl group. Medium was then removed, and fresh media containing test compounds and inhibitors where indicated were added. Fluorescence was measured every 0.6 s for 2 min using an inverted Leica TCS SP2 AOBS laser scanning confocal microscope with a 10× objective. Image analysis was performed using Leica LCS software, and fluorescence of every cell in each field was measured. On average, 68.2 ± 11.1 cells were separately analyzed per condition in each experiment. Cells exhibiting an increase of fluorescence at

least 2 times that of background, followed by a decrease in fluorescence and another increase in fluorescence, were scored as positive for calcium oscillations. Each condition was performed in duplicate within the experiment, and data shown are representative of at least three independent experiments.

Cell viability assay

BMDMs were seeded in 96-well plates at 5.0×10^4 cells per cm^2 and grown for 24 h. Cells were washed and incubated with medium with or without compounds as indicated for 24 h. MTS/PMS solution was then added to each well to a final concentration of 333 μg/ml MTS and 25 μmol/l PMS. After incubation for 2 h at 37°C, the absorbance at 490 nm was recorded using a Molecular Devices VersaMax microplate reader. Correlation between macrophage number and formation of formazan product has been previously established (11). Each condition was performed in triplicate within the experiment, and data are representative of at least three independent experiments.

Apoptosis assay

BMDM were seeded in 6-well plates at 5.0×10^4 cells per cm^2 and grown for 24 h. Cells were then washed and incubated with medium containing compounds as indicated for 24 h. Cells were harvested using a rubber cell scraper and fixed in 70% cold ethanol for 30 min. Cells were then washed with DPBS and stained with 3 μmol/l propidium iodide in DPBS containing 0.1% Triton X-100 and 0.73 μmol/l RNase A. DNA content was analyzed by flow cytometry on the FL-3 channel with appropriate gating used to exclude debris and cellular aggregates. Ten thousand events were counted for analysis. Each condition was performed in triplicate within the experiment and is representative of at least three independent experiments.

SK activity assay

BMDM were seeded in 60 mm plates at 5.0×10^4 cells per cm^2 and grown for 24 h. Cells were then washed and incubated with medium in the absence of M-CSF for 4 h. OxLDL (25 μg/ml) was then added for the time points indicated. Afterwards, cells were washed with DPBS and lysed with ice-cold solubilization buffer [50 mmol/l Tris-Cl, pH 8.0, 150 mmol/l NaCl, 1% Nonidet P-40 (IGEPAL CA-630), 10% glycerol, 154 nmol/l aprotinin, 2.90 μmol/l bestatin, 2.34 μmol/l leupeptin, 1.46 μmol/l pepstatin, 2.80 μmol/l trans-epoxysuccinyl-L-leucylamido(4-guanidino) butane (E-64), and 1 mmol/l sodium fluoride]. Lysates were centrifuged at 20,000 *g* for 10 min, and the protein content of supernatants was quantified by BCA protein assay. Equal amounts of protein were then incubated with 50 μmol/l sphingosine in 0.4% fatty acid-free BSA, 10 μCi of [^{32}P]ATP, and 100 mmol/l $MgCl_2$. The reaction was carried out for 30 min at 37°C and stopped by the addition of 20 μl of 1 N HCl and 800 μl of chloroform/methanol/HCl (100:200:1, v/v/v). After 10 min, 240 μl of chloroform and 240 μl of 2 mol/l KCl were added, and the samples were centrifuged at 3,000 *g* for 5 min. The aqueous layer was aspirated, and 250 μl of the organic layer were transferred to new glass tubes. The samples were evaporated under nitrogen gas and then resuspended in chloroform/methanol/HCl (100:200:1, v/v/v). Labeled S1P was resolved by TLC on G60 silica gel plates with 1-buthanol/methanol/acetic acid/water (80:20:10:20, v/v/v). Labeled S1P was then imaged and quantified using a Bio-Rad FX phosphor imager.

Statistical analyses

Categorical data (proportion of cells showing Ca^{2+} oscillations) were assessed with both Student's *t*-test and χ^2 test. Continuous data were assessed with Student's *t*-test. Comparisons showing *P* values < 0.05 were deemed significant.

RESULTS

LysoPC in oxLDL is not responsible for the generation of $[Ca^{2+}]_i$ oscillations

OxLDL and one of its components, lysoPC, have both been shown to induce an increase in $[Ca^{2+}]_i$ in macrophages (41–44). While 10 μmol/l lysoPC was able to elicit $[Ca^{2+}]_i$ oscillations in BMDMs to some extent, a considerably lower percentage of cells was positive for $[Ca^{2+}]_i$ oscillations compared with cells treated with oxLDL [the 25μg/ml of oxLDL used contains approximately 6 μmol/L lysoPC(45)] (**Fig. 1**). Furthermore, PC treatment elicited a response similar to that of lysoPC (Fig. 1). Hence, even though PC is converted to lysoPC during the LDL oxidation reaction (45), it is unlikely that the lysoPC content in oxLDL is responsible for the observed $[Ca^{2+}]_i$ oscillations.

Extracellular Ca^{2+} plays a partial role in the generation of $[Ca^{2+}]_i$ oscillations

An increase in $[Ca^{2+}]_i$ can be mediated by an influx of Ca^{2+} from the extracellular environment or from intracellular Ca^{2+} stores. To assess the contribution of extracellular Ca^{2+}, BMDMs were incubated in medium lacking Ca^{2+}. Under these conditions, the percentage of cells showing Ca^{2+} oscillations in response to oxLDL was reduced to less than half the level observed in cells incubated in media containing Ca^{2+} (**Fig. 2**). This indicates that while the presence of extracellular Ca^{2+} is required for the full effect of oxLDL, release from intracellular stores accounts for much of the observed $[Ca^{2+}]_i$ oscillations.

Thapsigargin blocks oxLDL-generated $[Ca^{2+}]_i$ oscillations

During the course of a Ca^{2+} transient, the release of calcium from stores is followed by reuptake via a number of pumps and exchangers that remove Ca^{2+} from the cytoplasm. SERCA is one of the pumps that returns Ca^{2+} from the cytoplasm to the ER (46). Thapsigargin, an epoxide derivative that selectively prevents Ca^{2+} binding to SERCA

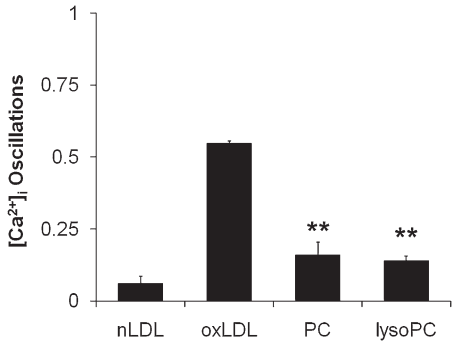

Fig. 1. LysoPC in oxLDL is not responsible for the generation of $[Ca^{2+}]_i$ oscillations. Calcium mobilization was visualized using fluo-4-AM and confocal fluorescence microscopy. After incubation with fluo-4-AM, BMDMs were washed, and media containing either nLDL (25 μg/ml), oxLDL (25 μg/ml), PC (10 μmol/l), or lysoPC (10 μmol/l) was added at time 0. Fluorescence values as a function of time were measured for every cell in the field, and cells positive for $[Ca^{2+}]_i$ oscillations are expressed as a fraction of total cells. ** $P < 0.01$ compared with cells treated with oxLDL.

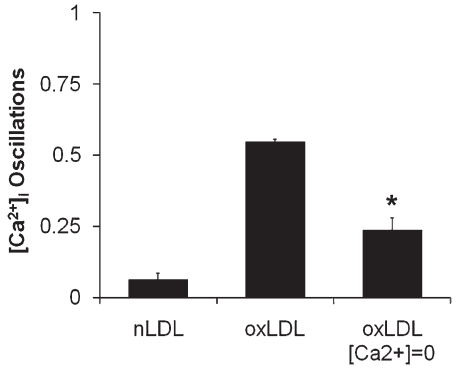

Fig. 2. Extracellular Ca^{2+} plays a partial role in the generation of $[Ca^{2+}]_i$ oscillations. Calcium mobilization was visualized using fluo-4-AM and confocal fluorescence microscopy. After preincubation with fluo-4-AM, BMDMs were washed, and nLDL or oxLDL (both 25 μg/ml) in media containing Ca^{2+} or oxLDL (25 μg/ml) in Ca^{2+}-free media was added at time 0. Fluorescence values as a function of time were measured for every cell in the field, and cells positive for $[Ca^{2+}]_i$ oscillations are expressed as a fraction of total cells. * $P < 0.05$ compared with cells treated with nLDL.

(47–49), completely blocked oxLDL-generated $[Ca^{2+}]_i$ oscillations (**Fig. 3**). This suggests that SERCA is responsible for Ca^{2+} reuptake to produce $[Ca^{2+}]_i$ oscillations.

Inhibition of phospholipase C or ryanodine receptor does not block oxLDL-mediated macrophage survival

Two well-studied mechanisms of Ca^{2+} release from intracellular stores involve inositol-1,4,5-triphosphate receptors (IP_3Rs) and ryanodine receptors (RyRs). Activation of phospholipase C (PLC) results in the conversion of phosphatidylinositol-4,5-bisphosphate to diacylglycerol and IP_3. The IP_3 stimulates IP_3R-mediated Ca^{2+} release from the ER. U-73122 is a selective inhibitor of PLC in this pathway (IC_{50} ~3 μmol/L) (50). Inhibition of PLC by U-73122 did not selectively inhibit oxLDL's prosurvival effect (**Fig. 4A**), in that it also decreased survival in control cells incubated without oxLDL. Dantrolene inhibits Ca^{2+} release from RyR channels

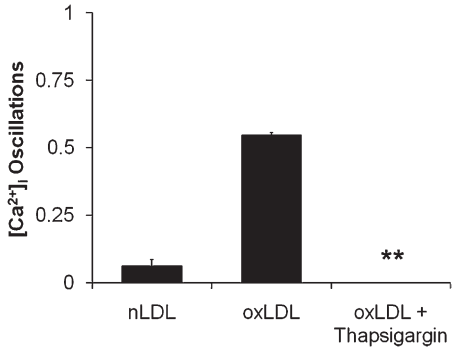

Fig. 3. Thapsigargin blocks oxLDL-generated $[Ca^{2+}]_i$ oscillations. Calcium mobilization was visualized using fluo-4-AM and confocal fluorescence microscopy. After incubation with fluo-4-AM, BMDMs were washed, and media containing 25 μg/ml nLDL, oxLDL, or oxLDL + thapsigargin (1 μmol/l) was added at time 0. Fluorescence values as a function of time were measured for every cell in the field, and cells positive for $[Ca^{2+}]_i$ oscillations are expressed as a fraction of total cells. ** $P < 0.01$ compared with cells treated with oxLDL alone.

(51). Inhibition of RyR-mediated Ca^{2+} release with this drug also did not block oxLDL's prosurvival effect (Fig. 4B).

S1P generates $[Ca^{2+}]_i$ oscillations and promotes macrophage survival

S1P can act as a second messenger to induce Ca^{2+} mobilization within the cell (38, 39). We demonstrated that S1P can generate $[Ca^{2+}]_i$ oscillations in BMDMs within the same time frame and as effectively as oxLDL (**Fig. 5**). Furthermore, the same concentration of S1P promoted BMDM survival (**Fig. 6A**) and blocked apoptosis (Fig. 6B) to the same extent as oxLDL. S1P arises from the phosphorylation of sphingosine by SK (36). It has been previously reported that oxLDL can activate SK in SMCs (52, 53), suggesting that the induction of $[Ca^{2+}]_i$ oscillations by oxLDL in BMDM might be mediated by its ability to increase phosphorylation of sphingosine.

SK is activated in response to oxLDL

To determine if oxLDL can activate SK in BMDMs, we used an in vitro kinase assay to measure the ability of cell

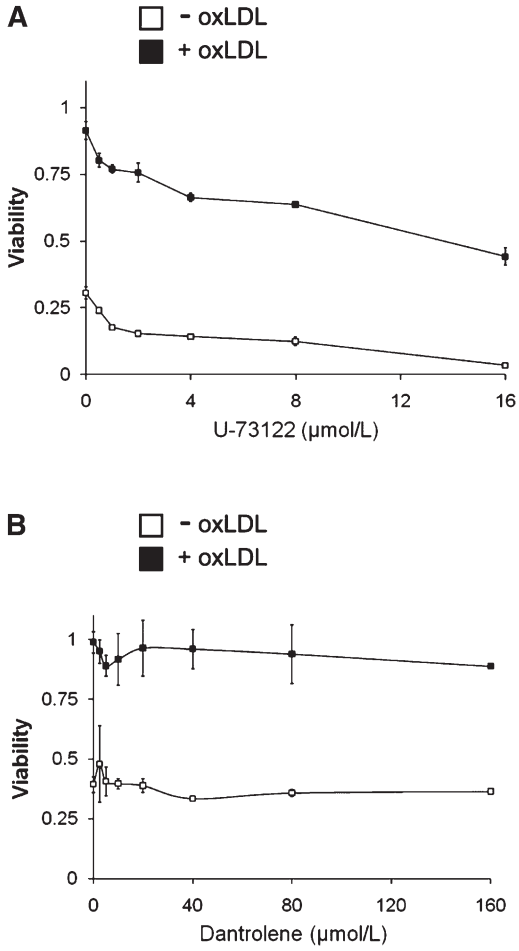

Fig. 4. Inhibition of PLC or RyR does not block oxLDL-mediated macrophage survival. A: BMDMs were washed and incubated with media alone or oxLDL (25 μg/ml) in the presence U-73122 or dantrolene at the concentrations indicated for 24 h. B: Viability was measured by the bioreduction of MTS and expressed as a ratio normalized to absorbance values of cells cultured in 10% M-CSF conditioned media.

lysates to phosphorylate sphingosine. There was a 1.5-fold increase in SK activity almost immediately after the addition of oxLDL (**Fig. 7**). This rapid activation of SK lends plausibility to the suggestion it could be a mechanism for mediating the $[Ca^{2+}]_i$ oscillations observed in response to oxLDL.

Inhibition of SK blocks oxLDL-mediated $[Ca^{2+}]_i$ oscillation and macrophage survival

To test if SK activation is required for the ability of oxLDL to induce $[Ca^{2+}]_i$ oscillation, we used a selective inhibitor of SK (54). Figure 7 shows that this compound effectively blocks SK activation by oxLDL. It also completely blocked oxLDL-generated $[Ca^{2+}]_i$ oscillations (**Fig. 8**) and oxLDL-mediated macrophage survival (**Fig. 9**). These results strongly suggest that oxLDL-induced Ca^{2+} mobilization is mediated by increased generation of S1P via SK activation.

DISCUSSION

A number of groups have reported that oxLDL induces an increase in $[Ca^{2+}]_i$ (41–44), and our studies extend this observation by demonstrating that at least in macrophages, this is an oscillatory increase. These oscillations involved Ca^{2+} release from intracellular stores and required SERCA to return cytosolic Ca^{2+} to the ER. S1P is known to induce intracellular calcium release in other cells (37), and we found it to be as effective as oxLDL at inducing $[Ca^{2+}]_i$ oscillations in BMDM. The addition of oxLDL resulted in an almost immediate activation of SK, which is the major cellular pathway to production of S1P.

Inhibition of SK activation blocked not only oxLDL-generated $[Ca^{2+}]_i$ oscillations but also oxLDL-mediated macrophage survival. This links Ca^{2+} signaling with the prosurvival effects of oxLDL. Delivery of S1P by oxLDL itself is unlikely because S1P is lost during the oxidation process (55). Furthermore, native LDL, which contains significant amounts of S1P (55), does not elicit a Ca^{2+} response similar to S1P, suggesting that endogenous production, perhaps in the plasma membrane, may be required to induce calcium oscillation (56). Our results do not exclude a role for other components of oxLDL, such as oxysterols, in stimulating intracellular $[Ca^{2+}]_i$ oscillations. However, the fact that the effect of oxLDL was mimicked by exogenous S1P and inhibited by an SK inhibitor suggests that S1P plays a major role. In addition, a recent study in U937 macrophages found that increased intracellular Ca^{2+}in response to 7β-hydroxycholesterol was mediated by influx of extracellular Ca^{2+} and was nonoscillatory (57). Both of these features are different from our findings with oxLDL-induced Ca^{2+} signaling in BMDM.

The exact mechanism in which S1P mediates Ca^{2+} mobilization is still uncertain. Ca^{2+} release mediated by S1P occurs independently of IP_3Rs and RyRs (58). One possible candidate is SCaMPER (for sphingolipid Ca^{2+} release mediating protein of the ER) (58). SCaMPER is a 181 amino acid protein that was first shown to mediate sphingolipid-gated Ca^{2+} release from intracellular stores in *Xenopus laevis* oocytes. More recently, antisense knockdown of SCaMPER mRNA was shown to substantially reduce sphingolipid-induced calcium release in human and rat cardiomyocytes (59). However, SCaMPER shares no similarity to

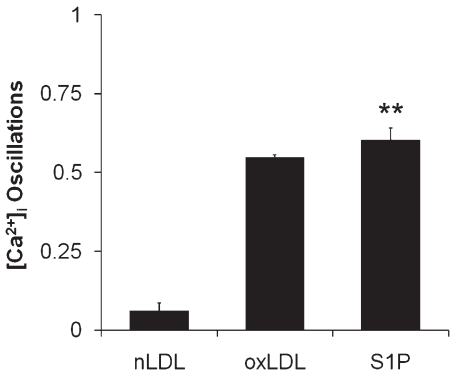

Fig. 5. S1P generates $[Ca^{2+}]_i$ oscillations. Calcium mobilization was visualized using fluo-4-AM and confocal fluorescence microscopy. After incubation with fluo-4-AM, BMDMs were washed, and media containing either nLDL (25 μg/ml), oxLDL (25 μg/ml), or S1P (30 μmol/l) was added at time 0. Fluorescence values as a function of time were measured for every cell in the field, and cells positive for $[Ca^{2+}]_i$ oscillations are expressed as a fraction of total cells. ** $P < 0.01$ compared with cells treated with nLDL.

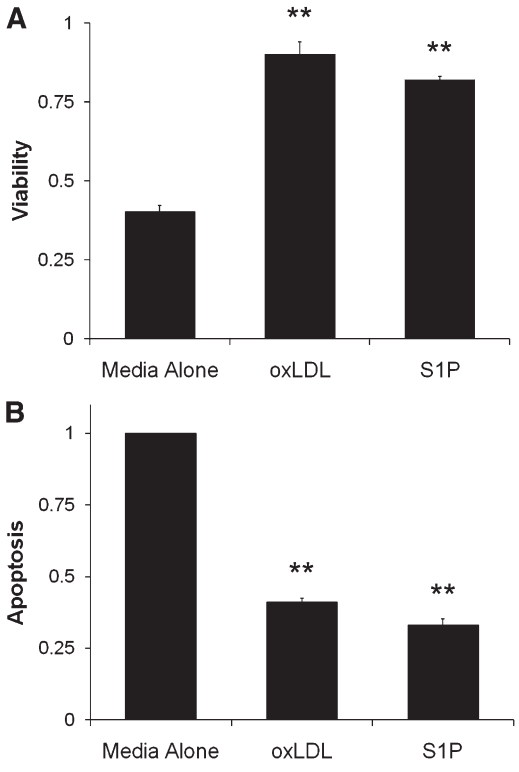

Fig. 6. S1P promotes macrophage survival. BMDMs were washed and incubated with media alone, oxLDL (25 μg/ml), or S1P (30 μmol/l) for 24 h. A: Viability was measured by the bioreduction of MTS and expressed as a ratio of normalized to absorbance values of cells cultured in 10% M-CSF conditioned media. B: Apoptosis was assessed by measuring the percentage of cells with subdiploid DNA. Data are expressed as a ratio of normalized to fluorescence values of cells cultured in the absence of M-CSF. ** $P < 0.01$ compared with cells treated with media alone.

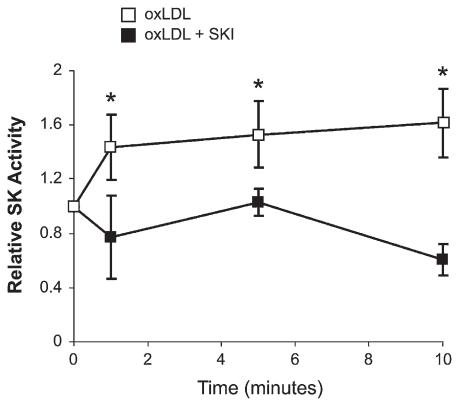

Fig. 7. SK is activated in response to oxLDL. BMDM were washed and incubated in medium without M-CSF for 4 h. OxLDL (25 μg/ml in medium without M-CSF) or oxLDL + SKI (30 μmol/l) was then added for the time periods indicated. SK activity was assessed by measuring the ability of lysates to phosphorylate sphingosine with an in vitro kinase assay. Data are normalized to values of cells at time 0. * $P < 0.05$ compared with cells at time 0.

any other known $[Ca^{2+}]_i$ channels and is a small protein with only one transmembrane domain (58). Thus, it is unlikely to itself be a Ca^{2+} channel. Furthermore, a study showed that there is little correlation between its intracellular location and that of known $[Ca^{2+}]_i$ stores (60).

We recently reported that oxLDL-mediated $[Ca^{2+}]_i$ oscillations lead to activation of the Ca^{2+}/calmodulin-dependent kinase, eEF2 kinase (16). Both the increase in $[Ca^{2+}]_i$ oscillations and the activation of eEF2 kinase were blocked by BAPTA-AM, an intracellular Ca^{2+} chelator. Addition of oxLDL also resulted in the phosphorylation of eEF2, the only known substrate of eEF2 kinase. The eEF2 kinase selective inhibitors TS-4 and TX-1918 blocked the ability of oxLDL to promote survival of BMDMs. Withdrawal of M-CSF resulted in the activation of p38 mitogen-activated protein kinase (MAPK), an effect that is blocked with the addition of oxLDL, and eEF2 kinase can be negatively regulated by p38 MAPK. Together, these results indicated that oxLDL can positively regulate eEF2 kinase activity by both *1*) generating an oscillatory increase in $[Ca^{2+}]_i$ and *2*) inhibiting its negative regulation by p38 MAPK. The only known substrate of eEF2K is eEF2, a monomeric GTPase that regulates peptide chain elongation. Phosphorylation of eEF2 inhibits its activity, thereby reducing the rate of protein synthesis. In keeping with its ability to activate eEF2K, addition of oxLDL results in a decrease in overall protein synthesis in BMDMs (16). Paradoxically, this effect of eEF2K activation has been shown to result in increased viability of cells under conditions of metabolic stress (e.g., growth factor withdrawal).

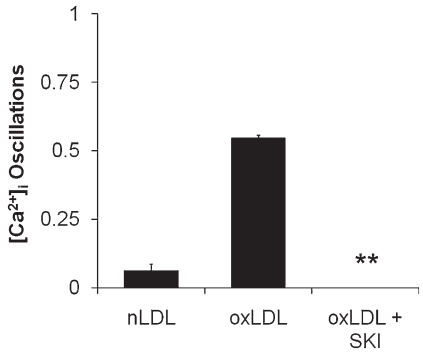

Fig. 8. Inhibition of SK blocks oxLDL-generated $[Ca^{2+}]_i$ oscillations. Calcium mobilization was visualized using fluo-4-AM and confocal fluorescence microscopy. After incubation with fluo-4-AM, BMDMs were washed, and media containing nLDL (25 μg/ml), oxLDL (25 μg/ml), or oxLDL (25 μg/ml) + SKI (30 μmol/l) was added at time 0. Fluorescence values as a function of time were measured for every cell in the field, and cells positive for $[Ca^{2+}]_i$ oscillations are expressed as a fraction of total cells. ** $P < 0.01$ compared with cells treated with oxLDL alone.

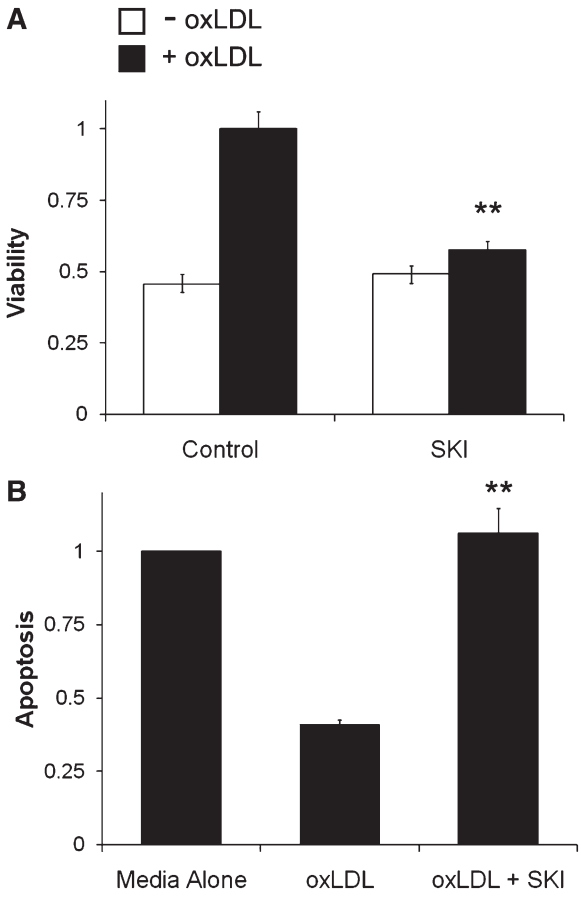

Fig. 9. Inhibition of SK blocks oxLDL-mediated macrophage survival. BMDMs were washed and incubated with media alone or oxLDL (25 μg/ml) in the presence or absence of SKI (30 μmol/l) for 24 h. A: Viability was measured by the bioreduction of MTS and expressed as a ratio of normalized to absorbance values of cells cultured in 10% M-CSF conditioned media. B: Apoptosis was assessed by measuring the percentage of cells with subdiploid DNA. Data are expressed as a ratio normalized to fluorescence values of cells cultured in the absence of M-CSF. ** $P < 0.01$ compared with cells treated with oxLDL alone.

The results described herein extend our previous observations and suggest a model in which oxLDL activates SK, triggering S1P-mediated oscillatory Ca^{2+} release from intracellular stores, which in turn leads to activation of eEF2K and energy conservation via inhibition of protein synthesis, culminating in increased macrophage survival.

REFERENCES

1. Ross, R. 1999. Atherosclerosis–an inflammatory disease. *N. Engl. J. Med.* **340:** 115–126.
2. Libby, P., and P. Theroux. 2005. Pathophysiology of coronary artery disease. *Circulation.* **111:** 3481–3488.
3. Rosenfeld, M. E., and R. Ross. 1990. Macrophage and smooth muscle cell proliferation in atherosclerotic lesions of WHHL and comparably hypercholesterolemic fat-fed rabbits. *Arteriosclerosis.* **10:** 680–687.
4. Gordon, D., M. A. Reidy, E. P. Benditt, and S. M. Schwartz. 1990. Cell proliferation in human coronary arteries. *Proc. Natl. Acad. Sci. USA.* **87:** 4600–4604.
5. Spagnoli, L. G., A. Orlandi, and G. Santeusanio. 1991. Foam cells of the rabbit atherosclerotic plaque arrested in metaphase by colchicine show a macrophage phenotype. *Atherosclerosis.* **88:** 87–92.
6. Rekhter, M. D., and D. Gordon. 1995. Active proliferation of different cell types, including lymphocytes, in human atherosclerotic plaques. *Am. J. Pathol.* **147:** 668–677.
7. Quinn, M. T., S. Parthasarathy, L. G. Fong, and D. Steinberg. 1987. Oxidatively modified low density lipoproteins: a potential role in recruitment and retention of monocyte/macrophages during atherogenesis. *Proc. Natl. Acad. Sci. USA.* **84:** 2995–2998.
8. Parthasarathy, S., M. T. Quinn, and D. Steinberg. 1988. Is oxidized low density lipoprotein involved in the recruitment and retention of monocyte/macrophages in the artery wall during the initiation of atherosclerosis? *Basic Life Sci.* **49:** 375–380.
9. Yui, S., T. Sasaki, A. Miyazaki, S. Horiuchi, and M. Yamazaki. 1993. Induction of murine macrophage growth by modified LDLs. *Arterioscler. Thromb.* **13:** 331–337.
10. Biwa, T., H. Hakamata, M. Sakai, A. Miyazaki, H. Suzuki, T. Kodama, M. Shichiri, and S. Horiuchi. 1998. Induction of murine macrophage growth by oxidized low density lipoprotein is mediated by granulocyte macrophage colony-stimulating factor. *J. Biol. Chem.* **273:** 28305–28313.
11. Martens, J. S., N. E. Reiner, P. Herrera-Velit, and U. P. Steinbrecher. 1998. Phosphatidylinositol 3-kinase is involved in the induction of macrophage growth by oxidized low density lipoprotein. *J. Biol. Chem.* **273:** 4915–4920.
12. Martens, J. S., M. Lougheed, A. Gomez-Munoz, and U. P. Steinbrecher. 1999. A modification of apolipoprotein B accounts for most of the induction of macrophage growth by oxidized low density lipoprotein. *J. Biol. Chem.* **274:** 10903–10910.
13. Hamilton, J. A., D. Myers, W. Jessup, F. Cochrane, R. Byrne, G. Whitty, and S. Moss. 1999. Oxidized LDL can induce macrophage survival, DNA synthesis, and enhanced proliferative response to CSF-1 and GM-CSF. *Arterioscler. Thromb. Vasc. Biol.* **19:** 98–105.
14. Hundal, R. S., B. S. Salh, J. W. Schrader, A. Gomez-Munoz, V. Duronio, and U. P. Steinbrecher. 2001. Oxidized low density lipoprotein inhibits macrophage apoptosis through activation of the PI 3-kinase/PKB pathway. *J. Lipid Res.* **42:** 1483–1491.
15. Hundal, R. S., A. Gomez-Munoz, J. Y. Kong, B. S. Salh, A. Marotta, V. Duronio, and U. P. Steinbrecher. 2003. Oxidized low density lipoprotein inhibits macrophage apoptosis by blocking ceramide generation, thereby maintaining protein kinase B activation and Bcl-XL levels. *J. Biol. Chem.* **278:** 24399–24408.
16. Chen, J. H., M. Riazy, E. M. Smith, C. G. Proud, U. P. Steinbrecher, and V. Duronio. 2009. Oxidized LDL-mediated macrophage survival involves elongation factor-2 kinase. *Arterioscler. Thromb. Vasc. Biol.* **29:** 92–98.
17. Berridge, M. J., M. D. Bootman, and H. L. Roderick. 2003. Calcium signalling: dynamics, homeostasis and remodelling. *Nat. Rev. Mol. Cell Biol.* **4:** 517–529.
18. Berridge, M. J., P. Lipp, and M. D. Bootman. 2000. The versatility and universality of calcium signalling. *Nat. Rev. Mol. Cell Biol.* **1:** 11–21.
19. Berridge, M. J., M. D. Bootman, and P. Lipp. 1998. Calcium–a life and death signal. *Nature.* **395:** 645–648.
20. Randriamampita, C., and A. Trautmann. 2004. Ca^{2+} signals and T lymphocytes; "New mechanisms and functions in Ca^{2+} signalling. *Biol. Cell.* **96:** 69–78.
21. Zhong, F., M. C. Davis, K. S. McColl, and C. W. Distelhorst. 2006. Bcl-2 differentially regulates Ca^{2+} signals according to the strength of T cell receptor activation. *J. Cell Biol.* **172:** 127–137.
22. Meyer zu Heringdorf, D., H. Lass, I. Kuchar, R. Alemany, Y. Guo, M. Schmidt, and K. H. Jakobs. 1999. Role of sphingosine kinase in Ca^{2+} signalling by epidermal growth factor receptor. *FEBS Lett.* **461:** 217–222.
23. Alemany, R., D. Meyer zu Heringdorf, C. J. van Koppen, and K. H. Jakobs. 1999. Formyl peptide receptor signaling in HL-60 cells through sphingosine kinase. *J. Biol. Chem.* **274:** 3994–3999.
24. Melendez, A. J., and A. K. Khaw. 2002. Dichotomy of Ca^{2+} signals triggered by different phospholipid pathways in antigen stimulation of human mast cells. *J. Biol. Chem.* **277:** 17255–17262.
25. Choi, O. H., J. H. Kim, and J. P. Kinet. 1996. Calcium mobilization via sphingosine kinase in signalling by the Fc epsilon RI antigen receptor. *Nature.* **380:** 634–636.
26. Melendez, A., R. A. Floto, D. J. Gillooly, M. M. Harnett, and J. M. Allen. 1998. FcgammaRI coupling to phospholipase D initiates sphingosine kinase-mediated calcium mobilization and vesicular trafficking. *J. Biol. Chem.* **273:** 9393–9402.
27. Spiegel, S., and A. H. Merrill, Jr. 1996. Sphingolipid metabolism and cell growth regulation. *FASEB J.* **10:** 1388–1397.
28. Cuvillier, O. 2002. Sphingosine in apoptosis signaling. *Biochim. Biophys. Acta.* **1585:** 153–162.
29. Maceyka, M., S. G. Payne, S. Milstien, and S. Spiegel. 2002. Sphingosine kinase, sphingosine-1-phosphate, and apoptosis. *Biochim. Biophys. Acta.* **1585:** 193–201.
30. Olivera, A., T. Kohama, L. Edsall, V. Nava, O. Cuvillier, S. Poulton, and S. Spiegel. 1999. Sphingosine kinase expression increases intracellular sphingosine-1-phosphate and promotes cell growth and survival. *J. Cell Biol.* **147:** 545–558.
31. Van Brocklyn, J. R., M. J. Lee, R. Menzeleev, A. Olivera, L. Edsall, O. Cuvillier, D. M. Thomas, P. J. Coopman, S. Thangada, C. H. Liu, et al. 1998. Dual actions of sphingosine-1-phosphate: extracellular through the Gi-coupled receptor Edg-1 and intracellular to regulate proliferation and survival. *J. Cell Biol.* **142:** 229–240.
32. Olivera, A., and S. Spiegel. 1993. Sphingosine-1-phosphate as second messenger in cell proliferation induced by PDGF and FCS mitogens. *Nature.* **365:** 557–560.
33. Edsall, L. C., G. G. Pirianov, and S. Spiegel. 1997. Involvement of sphingosine 1-phosphate in nerve growth factor-mediated neuronal survival and differentiation. *J. Neurosci.* **17:** 6952–6960.
34. Xu, C. B., Y. Zhang, E. Stenman, and L. Edvinsson. 2002. D-erythro-N,N-dimethylsphingosine inhibits bFGF-induced proliferation of cerebral, aortic and coronary smooth muscle cells. *Atherosclerosis.* **164:** 237–243.
35. Pitson, S. M., P. Xia, T. M. Leclercq, P. A. Moretti, J. R. Zebol, H. E. Lynn, B. W. Wattenberg, and M. A. Vadas. 2005. Phosphorylation-dependent translocation of sphingosine kinase to the plasma membrane drives its oncogenic signalling. *J. Exp. Med.* **201:** 49–54.
36. Hannun, Y. A., C. Luberto, and K. M. Argraves. 2001. Enzymes of sphingolipid metabolism: from modular to integrative signaling. *Biochemistry.* **40:** 4893–4903.
37. Alvarez, S. E., S. Milstien, and S. Spiegel. 2007. Autocrine and paracrine roles of sphingosine-1-phosphate. *Trends Endocrinol. Metab.* **18:** 300–307.
38. Meyer Zu Heringdorf, D. 2004. Lysophospholipid receptor-dependent and -independent calcium signaling. *J. Cell. Biochem.* **92:** 937–948.
39. Meyer zu Heringdorf, D., K. Liliom, M. Schaefer, K. Danneberg, J. H. Jaggar, G. Tigyi, and K. H. Jakobs. 2003. Photolysis of intracellular caged sphingosine-1-phosphate causes Ca^{2+} mobilization independently of G-protein-coupled receptors. *FEBS Lett.* **554:** 443–449.
40. Stanley, E. R., and P. M. Heard. 1977. Factors regulating macrophage production and growth. Purification and some properties of the colony stimulating factor from medium conditioned by mouse L cells. *J. Biol. Chem.* **252:** 4305–4312.
41. Matsumura, T., M. Sakai, S. Kobori, T. Biwa, T. Takemura, H. Matsuda, H. Hakamata, S. Horiuchi, and M. Shichiri. 1997. Two intracellular signaling pathways for activation of protein kinase C are involved in oxidized low-density lipoprotein-induced macrophage growth. *Arterioscler. Thromb. Vasc. Biol.* **17:** 3013–3020.
42. Schackelford, R. E., U. K. Misra, K. Florine-Casteel, S. F. Thai, S. V. Pizzo, and D. O. Adams. 1995. Oxidized low density lipoprotein suppresses activation of NF kappa B in macrophages via a pertussis toxin-sensitive signaling mechanism. *J. Biol. Chem.* **270:** 3475–3478.
43. Fueller, M., D. A. Wang, G. Tigyi, and W. Siess. 2003. Activation of human monocytic cells by lysophosphatidic acid and sphingosine-1-phosphate. *Cell. Signal.* **15:** 367–375.

44. Han, C. Y., S. Y. Park, and Y. K. Pak. 2000. Role of endocytosis in the transactivation of nuclear factor-kappaB by oxidized low-density lipoprotein. *Biochem. J.* **350:** 829–837.
45. Steinbrecher, U. P., S. Parthasarathy, D. S. Leake, J. L. Witztum, and D. Steinberg. 1984. Modification of low density lipoprotein by endothelial cells involves lipid peroxidation and degradation of low density lipoprotein phospholipids. *Proc. Natl. Acad. Sci. USA.* **81:** 3883–3887.
46. Pozzan, T., R. Rizzuto, P. Volpe, and J. Meldolesi. 1994. Molecular and cellular physiology of intracellular calcium stores. *Physiol. Rev.* **74:** 595–636.
47. Inesi, G., and Y. Sagara. 1992. Thapsigargin, a high affinity and global inhibitor of intracellular Ca^{2+} transport ATPases. *Arch. Biochem. Biophys.* **298:** 313–317.
48. Sagara, Y., F. Fernandez-Belda, L. de Meis, and G. Inesi. 1992. Characterization of the inhibition of intracellular Ca^{2+} transport ATPases by thapsigargin. *J. Biol. Chem.* **267:** 12606–12613.
49. Sagara, Y., J. B. Wade, and G. Inesi. 1992. A conformational mechanism for formation of a dead-end complex by the sarcoplasmic reticulum ATPase with thapsigargin. *J. Biol. Chem.* **267:** 1286–1292.
50. Yule, D. I., and J. A. Williams. 1992. U73122 inhibits Ca2+ oscillations in response to cholecystokinin and carbachol but not to JMV-180 in rat pancreatic acinar cells. *J. Biol. Chem.* **267:** 13830–13835.
51. Zhao, F., P. Li, S. R. Chen, C. F. Louis, and B. R. Fruen. 2001. Dantrolene inhibition of ryanodine receptor Ca^{2+} release channels. Molecular mechanism and isoform selectivity. *J. Biol. Chem.* **276:** 13810–13816.
52. Auge, N., V. Garcia, F. Maupas-Schwalm, T. Levade, R. Salvayre, and A. Negre-Salvayre. 2002. Oxidized LDL-induced smooth muscle cell proliferation involves the EGF receptor/PI-3 kinase/Akt and the sphingolipid signaling pathways. *Arterioscler. Thromb. Vasc. Biol.* **22:** 1990–1995.
53. Auge, N., M. Nikolova-Karakashian, S. Carpentier, S. Parthasarathy, A. Negre-Salvayre, R. Salvayre, A. H. Merrill, Jr., and T. Levade. 1999. Role of sphingosine 1-phosphate in the mitogenesis induced by oxidized low density lipoprotein in smooth muscle cells via activation of sphingomyelinase, ceramidase, and sphingosine kinase. *J. Biol. Chem.* **274:** 21533–21538.
54. French, K. J., R. S. Schrecengost, B. D. Lee, Y. Zhuang, S. N. Smith, J. L. Eberly, J. K. Yun, and C. D. Smith. 2003. Discovery and evaluation of inhibitors of human sphingosine kinase. *Cancer Res.* **63:** 5962–5969.
55. Kimura, T., K. Sato, A. Kuwabara, H. Tomura, M. Ishiwara, I. Kobayashi, M. Ui, and F. Okajima. 2001. Sphingosine 1-phosphate may be a major component of plasma lipoproteins responsible for the cytoprotective actions in human umbilical vein endothelial cells. *J. Biol. Chem.* **276:** 31780–31785.
56. Itagaki, K., J. K. Yun, J. A. Hengst, A. Yatani, C. J. Hauser, Z. Spolarics, and E. A. Deitch. 2007. Sphingosine 1-phosphate has dual functions in the regulation of endothelial cell permeability and Ca^{2+} metabolism. *J. Pharmacol. Exp. Ther.* **323:** 186–191.
57. Lordan, S., N. M. O'Brien, and J. J. Mackrill. 2009. The role of calcium in apoptosis induced by 7beta-hydroxycholesterol and cholesterol-5beta,6beta-epoxide. *J. Biochem. Mol. Toxicol.* **23:** 324–332.
58. Mao, C., S. H. Kim, J. S. Almenoff, X. L. Rudner, D. M. Kearney, and L. A. Kindman. 1996. Molecular cloning and characterization of SCaMPER, a sphingolipid Ca^{2+} release-mediating protein from endoplasmic reticulum. *Proc. Natl. Acad. Sci. USA.* **93:** 1993–1996.
59. Cavalli, A. L., N. W. O'Brien, S. B. Barlow, R. Betto, C. C. Glembotski, P. T. Palade, and R. A. Sabbadini. 2003. Expression and functional characterization of SCaMPER: a sphingolipid-modulated calcium channel of cardiomyocytes. *Am. J. Physiol. Cell Physiol.* **284:** C780–C790.
60. Schnurbus, R., D. de Pietri Tonelli, F. Grohovaz, and D. Zacchetti. 2002. Re-evaluation of primary structure, topology, and localization of Scamper, a putative intracellular Ca^{2+} channel activated by sphingosylphosphocholine. *Biochem. J.* **362:** 183–189.